

# Azimuthal Asymmetry of Pion-Meson Emission around the Projectile and Target Sides in Au+Au Collision at 1A GeV \*

WANG Ting-Ting(王婷婷)<sup>1,2</sup>, LÜ Ming(吕明)<sup>1,2</sup>, MA Yu-Gang(马余刚)<sup>1\*\*</sup>, FANG De-Qing(方德清)<sup>1</sup>,  
WANG Shan-Shan(王闪闪)<sup>1,3</sup>, ZHANG Guo-Qiang(张国强)<sup>1</sup>

<sup>1</sup>Shanghai Institute of Applied Physics, Chinese Academy of Sciences, Shanghai 201800

<sup>2</sup>University of Chinese Academy of Sciences, Beijing 100049

<sup>3</sup>Institute of Particle and Nuclear Physics, Henan Normal University, Xinxiang 453007

(Received 24 April 2015)

The ratio of the number of emitted pions from the target side to that from the projectile side at target rapidity within the reaction plane is investigated for the study of the pion dynamics with an isospin-dependent quantum molecular dynamic model. The results show that high-energy pions are emitted preferentially towards the target side and, therefore, they are freezed out at the early stage of the collision. By contrast, low-energy pions are emitted predominantly in the opposite direction, which means that they are emitted in later stage. This argument is based on the shadowing effect caused by the interaction of pions with the spectator matter in peripheral collisions at target or projectile rapidities. This phenomenon disappears in the central collision or at midrapidity due to the weaker shadowing effect. The calculated ratios are also compared with the experimental data.

PACS: 25.75.Dw, 25.75.Ld, 24.10.Lx

DOI: 10.1088/0256-307X/32/6/062501

High energy heavy ion collisions (HIC) provide an ideal tool to study the state of nuclear matter at higher energy densities. Due to the fast process of the collision, one can only detect the particles at freeze-out stage while the early stage information of HIC might be missed. To investigate the properties of nuclear matter at high density in the compression stage, one must find probes which are sensitive to the properties of this dense matter to gain information about nuclear matter under high density conditions. The pion meson, which is the most abundantly produced particle at relativistic energies, is an interesting probe of the hot and dense hadronic matter in heavy ion collisions.<sup>[1–3]</sup> Some observables have been found to be sensitive to the nuclear equation of state (EOS),<sup>[4]</sup> of which the pion multiplicity is one of them.<sup>[1,5,6]</sup> Meanwhile, experimental data of  $\pi$  analysis of streamer chamber events at the BEVALAC<sup>[2,7,8]</sup> was available and used to obtain the EOS information by the comparison with the dynamical models. One interesting observable, azimuthal anisotropy of pion emission in asymmetric heavy ion reactions was experimentally investigated by Gosset *et al.* and a preferential emission of charged pions away from the interaction zone towards the projectile side was observed. This result can be attributed to a stronger pion absorption by the heavier spectator remnant, i.e., an effect of shadowing by a large spectator nuclei.<sup>[9]</sup>

One observable for characterizing the quantitative anisotropy is using the ratio of the number of pions emitted to the projectile side and that to the target side within the reaction plane,<sup>[10]</sup> however, there are few theoretical studies to date. In this work, we study the above ratio of pion emission for the Au+Au colli-

sion at 1A GeV by a transport model, namely isospin-dependent quantum molecular dynamics (IQMD) and try to compare with the available data.

The quantum molecular dynamics (QMD) model is a transport model which is based on a many body theory to describe heavy ion collisions from low (dozens of MeV) to relativistic energy.<sup>[11]</sup> The IQMD, was extended from the QMD model, with considering the isospin effects. In the past decades, many applications have been successfully performed into nuclear physics studies with the help of IQMD. For instance, IQMD has been successfully applied to treat collective flow, multifragmentation, isospin effects in HIC, transport coefficient in HIC, giant monopole resonance, giant and pygmy dipole resonances, symmetry energy, and strangeness production.<sup>[12–23]</sup> In addition, nuclear modification factor and radial flow of protons for Au+Au collision at 1A GeV have been simulated with the IQMD model and it demonstrated that the soft equation of state with momentum-dependent interaction (MDI) can give an excellent description with the data.<sup>[24,25]</sup> In this context, we take the same soft EOS with MDI for the current simulation on projectile-target azimuthal asymmetry of pion emission in Au+Au collision at 1A GeV. For the details of the model, one can refer to Refs. [11,24,25].

To have a direct feeling on heavy ion collision evolution for 1A GeV Au+Au, we display Fig. 1 for the density contours for the impact parameter of 7 fm at 5, 10, 15, 20, 25 and 30 fm/c after time zero (which is the time instant when both nuclei have a distance projected to the beam axis of 2 times the nuclear radius) in our IQMD simulation. The different snapshots correspond to the effect of pion shadowing by

\*Supported by the National Natural Science Foundation of China under Grant Nos 11421505 and 11220101005, and the National Basic Research Program of China under Grant No 2014CB845401.

\*\*Corresponding author. Email: ygma@sinap.ac.cn

© 2015 Chinese Physical Society and IOP Publishing Ltd

spectator matter at different stages of the collision. In the early phase of the collision, saying at  $5 \text{ fm}/c$  in Fig. 1, pions which are detected around target rapidity (i.e., at backward angles as indicated by the arrows in Fig. 1) will be shadowed by the projectile spectator on one side and therefore exhibit flow to the other side. This apparent pion flow can be taken as a potentially powerful tool for exploring the nuclear dynamics and equation of state of nuclear matter.<sup>[26,27]</sup> In contrast, if pions freeze out at a late stage of the collision, saying after  $15 \text{ fm}/c$  in Fig. 1, they will be shadowed (at target rapidity) by the target spectator which results in an anti-flow-like configuration. Meanwhile, in a middle stage, e.g.,  $10 \text{ fm}/c$  in Fig. 1, the particles could be azimuthally symmetrically emitted around the projectile-target sides. The above antiflow behavior of pions is found to be pronounced in peripheral Au+Au collisions and vanishes in central collisions.<sup>[1]</sup> More details of the flow and antiflow can be found in Ref. [28] for the reaction of Au+Au at  $1.15 \text{ A GeV}$ . Theoretical studies of pion flow in the symmetric Au+Au system have been presented by Bass *et al.*<sup>[29]</sup> for  $1 \text{ A GeV}$  and by Li<sup>[30]</sup> for  $0.6\text{--}1.6 \text{ A GeV}$ . New theoretical studies can also be found by a recent ImQMD calculation.<sup>[31]</sup>

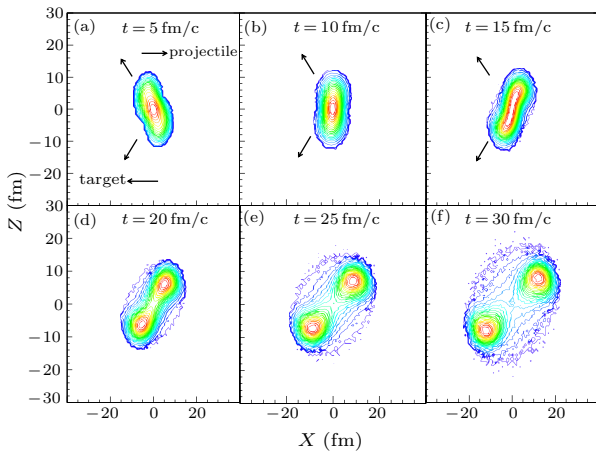
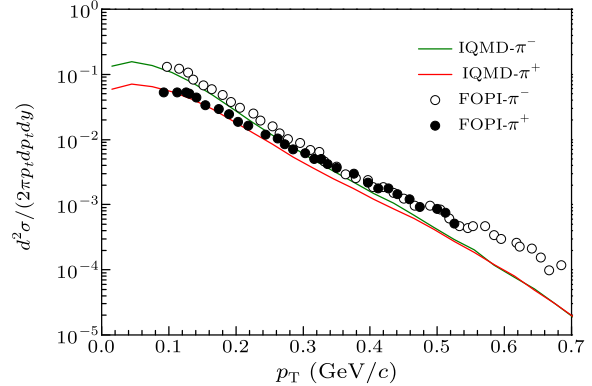


**Fig. 1.** (Color online) Sketch of Au+Au collision at  $1 \text{ A GeV}$  with an impact parameter of  $7 \text{ fm}$ . A soft EOS with MDI is used in our calculation. The snapshots are taken at  $5$  (a),  $10$  (b),  $15$  (c),  $20$  (d),  $25$  (e), and  $30 \text{ fm}/c$  (f). The left-side region between the left two arrows indicates a target rapidity region.

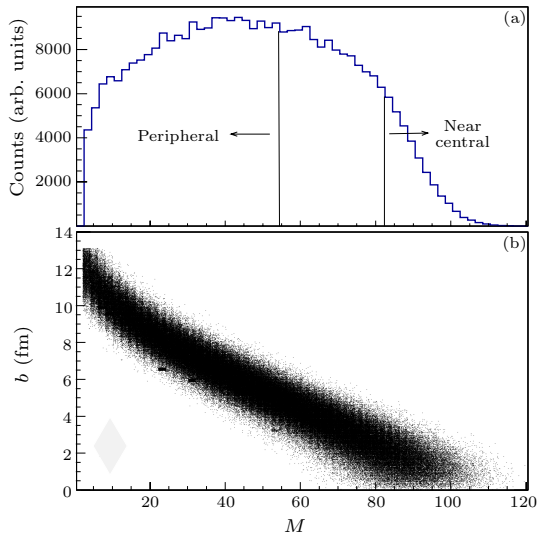
Pions are formed by the decay of the  $\Delta$  resonance (i.e.,  $\Delta \rightarrow N\pi$ ) (for the energy region of about  $1 \text{ A GeV}$ ) in the IQMD model.<sup>[29]</sup> After pions which are free or bound in a delta are produced, they may be reabsorbed by another nucleon forming a  $\Delta$  which may be absorbed in an inelastic collision or they may decay again producing another pion, i.e., (i) absorption:  $\pi N \rightarrow \Delta$ ,  $\Delta N \rightarrow NN$ ; and (ii) scattering (resorption):  $\pi N \rightarrow \Delta \rightarrow \pi N$ .

Figure 2 shows the transverse momentum ( $p_{\text{T}}$ ) spectra of charged pions under minimum bias trigger at midrapidity with the IQMD model together with the experimental data of the FOPI collaboration.<sup>[32]</sup> The slopes of our simulation are in a well agreement

with the experimental data for both positive and negative pions. In the region of low transverse momentum, the different trend of pions is attributed to the Coulomb potential of the charged pion interaction.



**Fig. 2.** (Color online) Comparison of pion transverse momentum distributions of our IQMD simulations with minimum bias trigger condition with the measured ones by the FOPI collaboration.<sup>[32]</sup>



**Fig. 3.** (Color online) (a) Multiplicity distribution of charged particles  $M$  for Au+Au collisions at  $1 \text{ A GeV}$  under the same condition as the Kaon spectrometer at GSI (Darmstadt)<sup>[10]</sup> with the large polar-angle triggered with a particle in the small polar-angle by the IQMD model. (b) The correlation between total multiplicity and impact parameter with the same condition given above in the IQMD model calculation.

For our purpose, it is convenient to transfer from the coordinates  $(p_z, p_{\text{T}}, \varphi)$  to the spherical coordinates  $(p, \theta, \varphi)$ , where  $\theta$  is the polar angle,  $\varphi$  is the azimuthal angle between the transverse momentum vector  $p_{\text{T}}$  and the  $p_x$ -axis (which lies in the reaction plane and is perpendicular to the beam axis), and  $\theta$  is the angle between the total momentum vector and the  $p_z$  axis.

As the experimental way, we determine the collision centrality using the charged particle multiplicity distribution in the IQMD model for the Au+Au collision with a minimum-bias impact parameter distribution at  $1 \text{ A GeV}$  incident energy. To make a

quantitative comparison with the experimental data, the charged particle multiplicity distribution is constructed in our simulation, which required a multiplicity number more than two is obtained with one particle in the large polar-angle ( $12^\circ \leq \theta_{\text{lab}} \leq 48^\circ$ ) triggered with another particle in the small polar-angle ( $\theta_{\text{lab}} = 44^\circ \pm 4^\circ$ ). Figure 3(a) shows that peripheral collisions are strongly suppressed by the trigger condition. As shown in the picture, we selected peripheral collision which has  $65 \pm 5\%$  of the area of the charged particle multiplicity distribution in the large polar angle range given above and the near central collisions which has  $14 \pm 4\%$  centrality, respectively, the same as the experimental condition. Figure 3(b) shows the correlation between the multiplicity and the impact parameter under the above trigger of  $M$ .

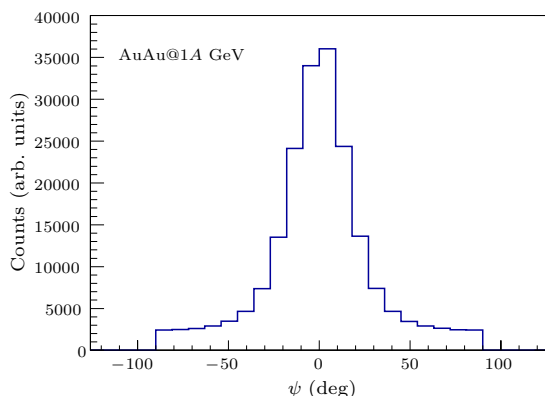


**Fig. 4.** (Color online) Event plane angle ( $\psi$ ) distribution in the polar angle  $0.5^\circ \leq \theta_{\text{lab}} \leq 5^\circ$  for Au+Au collisions at 1A GeV with the minimum bias impact parameter distribution by the IQMD model.

To simulate an event-by-event analysis of heavy-ion reactions at 1A GeV the same as the experiment, it is necessary to define a general reference frame for each event.<sup>[33]</sup> The event-plane method uses the event-plane angle determined from the observed collective flow itself as the approximate reaction plane.<sup>[15,16,33,34]</sup> The event plane angle is given as  $\psi = \arctan(Q_y/Q_x)$ , where  $Q_y = \sum_i \omega_i \cos(\varphi_i)$ , and  $Q_x = \sum_i \omega_i \sin(\varphi_i)$ , in which the sum runs over all the particles used in the reconstruction of the event plane. Here  $\varphi_i$  and  $\omega_i$  are the azimuthal angle and weight for particle  $i$ . We choose  $\omega_i = p_t$  for rapidity  $Y_i > 0.3$  and  $\omega_i = -p_t$  if  $Y_i < -0.3$ . Figure 4 shows the  $\psi$  distribution within the polar angle ( $0.5^\circ \leq \theta_{\text{lab}} \leq 5^\circ$ ). Most of the particles emitted in this angular range are spectator particles. Their phase space information is used to reconstruct the event plane. Once the event plane angle is available, the observed azimuthal angle  $\varphi$  for each particle with respect to the event plane can be calculated by  $\varphi = \varphi_i - \psi$ .

In previous works,<sup>[2,3]</sup> the observation of azimuthal anisotropy with a preferential emission of pions perpendicular to the reaction plane has been reported, i.e., the so-called squeeze-out behavior. This phenomenon takes place in mid-rapidity interaction zone where particles favor to be emitted out-of-plane and the in-plane emission is hindered due to the shad-

owing effect of the projectile and target spectators. In such an experimental observation, the determination of reaction plane is one of important points as mentioned above. In the present simulation, we obtain event plane in the above way, and then quantitatively compare the calculated azimuthal anisotropy with the experimental one. Theoretically, we compare the number of pions emitted in the reaction plane to the side of the projectile spectator ( $N_\pi(0)$ ) with the one on the opposite side ( $N_\pi(180)$ ). Here  $N_\pi(0)$  refers to the azimuthal angular in the range of  $-45^\circ < \varphi < 45^\circ$ , and  $N_\pi(180)$  refers to the azimuthal angular range of  $135^\circ < \varphi < 225^\circ$ . Thus  $N_\pi(0)$  denotes the projectile hemisphere and  $N_\pi(180)$  corresponds to the target hemisphere. In addition, the remnants  $45^\circ < \varphi < 135^\circ$  represent the out-of-plane emission, which is denoted as  $N_\pi(90)$ .

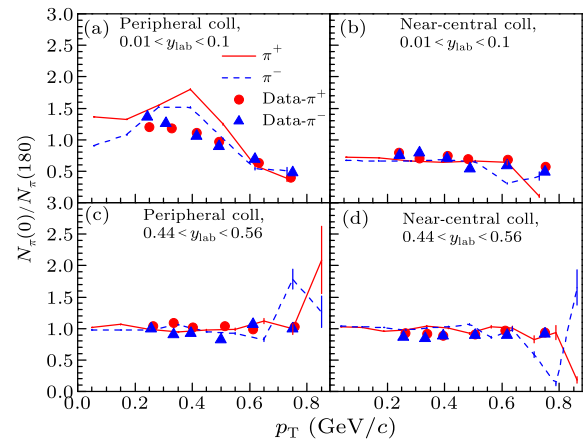


**Fig. 5.** (Color online) The ratio of pions emitted in the projectile side to the ones in the target side ( $N_\pi(0)/N_\pi(180)$ ) as a function of the total momentum  $p_T$ : (a) for peripheral collisions and target rapidity, (b) for the near central collisions at target rapidity, (c) for peripheral collisions and mid-rapidity, (d) for the near central collisions at mid-rapidity. Circles and triangles represent the data of  $\pi^+$  and  $\pi^-$ , respectively.<sup>[10]</sup> The solid and dashed lines represent our simulations of  $\pi^+$  and  $\pi^-$ .

The spectra of emitted pions can be obtained in the later stage of collisions, i.e., at 100 fm/c in the present simulation. The ratios of these pion spectra as a function of transverse momentum  $p_T$  can be directly obtained for peripheral (left panels) or near-central (right panels) collisions at target rapidity (upper panels) or mid-rapidity (bottom panels) as shown in Fig. 5. The results are also compared with the experimental data of the Kaon Spectrometer at the heavy-ion synchrotron SIS at GSI (Darmstadt)<sup>[10]</sup> in the figure. The trend of our simulation and the experimental data are quite similar. In Fig. 5(a), high energy pions above  $p_T$  of 0.5 GeV/c are preferentially emitted to the side of the target spectator. In contrary, low energy pions are slightly preferentially emitted to the side of the projectile spectator. This finding shows that high energy pions are shadowed by the projectile spectator, whereas the low energy pions are shadowed by the target spectator. In Fig. 5(b), the asymmetry becomes gradually weaken in near-central collisions at

target rapidity. This is consistent with Ref. [1] which proposed that the shadowing effect is found only in peripheral Au+Au collisions and strongly reduced for near central collisions.<sup>[1]</sup> We also find for near-central and peripheral collisions at mid-rapidity, the measured ratios are close to 1 as expected for symmetric systems in Figs. 5(c) and 5(d).

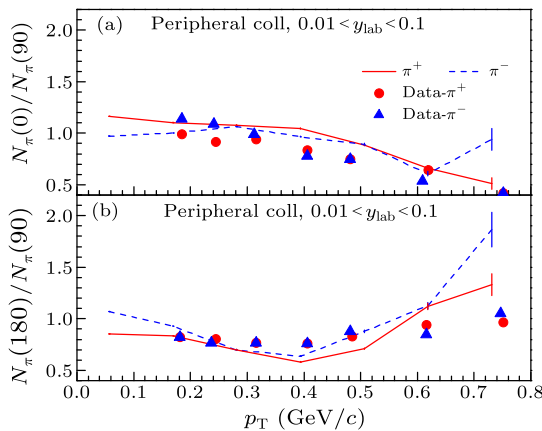


**Fig. 6.** (Color online) The ratio of pions emitted in the projectile side to the ones in out-of-plane ( $N_\pi(0)/N_\pi(90)$ ) (a) and that of pions emitted in the target side to the ones in out-of-plane ( $N_\pi(180)/N_\pi(90)$ ) (b) as a function of transverse momentum  $p_T$  in target rapidity. Circles and triangles represent the data of  $\pi^+$  and  $\pi^-$ , respectively.<sup>[10]</sup> The solid and dashed lines represent our simulations of  $\pi^+$  and  $\pi^-$ , respectively.

Next, we discuss in more details through comparing the yield of pions which are emitted in plane to those which are emitted perpendicular to the reaction plane. Figure 6 shows the ratio  $N_\pi(0)/N_\pi(90)$  and  $N_\pi(180)/N_\pi(90)$  as a function of  $p_T$  in peripheral collisions at target rapidity. Again, the data<sup>[10]</sup> was compared by our simulation. The ratios are both less than unity, which indicates that the transition of the ratio  $N_\pi(0)/N_\pi(180)$  (Fig. 5(a)) is not caused by an enhanced pion emission while rather by losses due to absorption or rescattering. Through comparing Fig. 5(a) with Fig. 6, we could extract indicated information on the emission time of pions as a function of their momentum. The ratio shows no asymmetry ( $N_\pi(0)/N_\pi(180) \approx 1$ ) at  $p_T \sim 0.5 \text{ GeV}/c$  in Fig. 5(a), whereas it clearly shows that both ratios of  $N_\pi(0)/N_\pi(90)$  and  $N_\pi(180)/N_\pi(90)$  at both projectile and target sides are less than 1 in Figs. 6(a) and 6(b). This finding shows that they are shadowed by both the target and the projectile spectators when pions are emitted at about  $10 \text{ fm}/c$  (see Fig. 1). In the region of high transverse momentum (above  $p_T$  of  $0.5 \text{ GeV}/c$ ), the ratio has a drop with increasing transverse momentum for pions emitted towards the projectile side (Fig. 6(a)), while on the target side the opposite trend is observed (Fig. 6(b)). This observation demonstrates that high transverse momentum pions are emitted at the early stage which are earlier than  $10 \text{ fm}/c$  in the present simulation. In contrast, low transverse momentum pions preferentially freeze out at later time.

In summary, we have investigated the pion emission in peripheral and near-central Au+Au collisions at  $1 \text{ A GeV}$  with the IQMD model. Firstly, we compare the transverse momentum ( $p_T$ ) spectra of charged pions obtained by the IQMD model with the FOPI experimental data, and we find they have a well agreement. Then, we have studied the ratio of the number of emitted pions from the target side to that from the projectile side at target rapidity within the reaction plane. It is observed that an obvious reduction of high  $p_T$  pion emission at the projectile side and while a slight reduction of low  $p_T$  pion emission at the target side. These results stem from that the projectile spectator is shielding the high energy pions to the projectile side, which means that the high energy pions are emitted at the early phase of the collision. However, low energy pions are shadowed by the target spectator, therefore, they freeze out at the later time.

## References

- [1] Stocker H, Greiner W, Scheid W et al 1978 *Z. Phys. A* **286** 121
- [2] Harris J, Bock R, Brockmann R, Sandoval A, Stock R and Stroebele H 1985 *Phys. Lett. B* **153** 377
- [3] Stocker H and Greiner W 1986 *Phys. Rep.* **137** 277
- [4] Li B A, Chen L W and Ko C M 2008 *Phys. Rep.* **464** 113
- [5] Danielewicz P 1979 *Nucl. Phys. A* **314** 465
- [6] Stocker H, Oglloblin A A et al 1981 *Z. Phys. A* **303** 259
- [7] Sandoval A, Stock R et al 1980 *Phys. Rev. Lett.* **45** 874
- [8] Stock R, Bock R et al 1982 *Phys. Rev. Lett.* **49** 1236
- [9] Gossset J, Valette O et al 1989 *Phys. Rev. Lett.* **62** 1251
- [10] Wagner A, Muntz C et al 2000 *Phys. Rev. Lett.* **85** 18
- [11] Aichelin J 1991 *Phys. Rep.* **202** 233
- [12] Hartnack C, Oeschler H, Leifels Y et al 2012 *Phys. Rep.* **510** 119
- [13] Kumar S and Ma Y G 2012 *Phys. Rev. C* **86** 051601(R)
- [14] Kumar S and Ma Y G 2013 *Nucl. Sci. Tech.* **24** 050509
- [15] Wang J, Ma Y G, Zhang G Q et al 2013 *Nucl. Sci. Tech.* **24** 030501
- [16] Wang J, Ma Y G et al 2014 *Phys. Rev. C* **90** 054601
- [17] Tao C, Ma Y G et al 2013 *Nucl. Sci. Tech.* **24** 030501
- [18] Tao C, Ma Y G et al 2013 *Phys. Rev. C* **88** 064615
- [19] Guo W J et al 2014 *Chin. Phys. Lett.* **31** 102501
- [20] Zhang Y X, Li Z X, Zhao K, Liu H and Tsang M B 2013 *Nucl. Sci. Tech.* **24** 050503
- [21] Feng Z Q 2013 *Nucl. Sci. Tech.* **24** 050504
- Feng Z Q 2015 *Nucl. Sci. Tech.* **26** S20512
- [22] Zhou C L, Ma Y G, Fang D Q et al 2014 *Nucl. Tech.* **37** 100516 (in Chinese)
- [23] Zhou C L, Ma Y G, Fang D Q et al 2014 *Phys. Rev. C* **90** 057601
- [24] Lv M, Ma Y G, Zhang G Q et al 2014 *Phys. Lett. B* **733** 105
- [25] Lyu M, Ma Y G, Zhang G Q et al 2014 *Nucl. Tech.* **37** 100517 (in Chinese)
- [26] Li B A, Bauer W and Bertsch G F 1991 *Phys. Rev. C* **44** 2095
- [27] Bass S A, Mattiello R, Stocker H et al 1993 *Phys. Lett. B* **302** 381
- [28] Kintner J C, Albergo S, Bieser F et al 1997 *Phys. Rev. Lett.* **78** 4165
- [29] Bass S A, Hartnack C, Stocker H et al 1995 *Phys. Rev. C* **51** 3343
- [30] Li B A 1994 *Nucl. Phys. A* **570** 797
- [31] Feng Z Q and Jin G M 2010 *Phys. Rev. C* **82** 044615
- [32] Pelte D, Hafele E, Best D et al 1997 *Z. Phys. A* **357** 215
- [33] Danielewicz P 1995 *Phys. Rev. C* **51** 716
- [34] Zhou F C, Cai X and Zhou D C 2014 *Chin. Phys. Lett.* **31** 072501